

Supporting Information for

**Synergetic polarization effect of protonation and Fe-doping toward
g-C₃N₄ with enhanced photocatalytic activity**

Xiaogang Liu^{*a}, Wenjie Chen^a, Wei Wang^b and Zhengbo Jiao^{*c}

a. College of Chemistry and Chemical Engineering, Xinyang Normal University, Xinyang, Henan 464000, P. R. China.

b. State Key Laboratory of High-efficiency Utilization of Coal and Green Chemical Engineering, Ningxia University, Yinchuan 750021, P. R. China.

c. Institute of Materials for Energy and Environment, and College of Material Science and Engineering, Qingdao University, Qingdao 266071, China

E-mail: lxg133298@163.com; jiaozhb@163.com

Additional figures and tables.

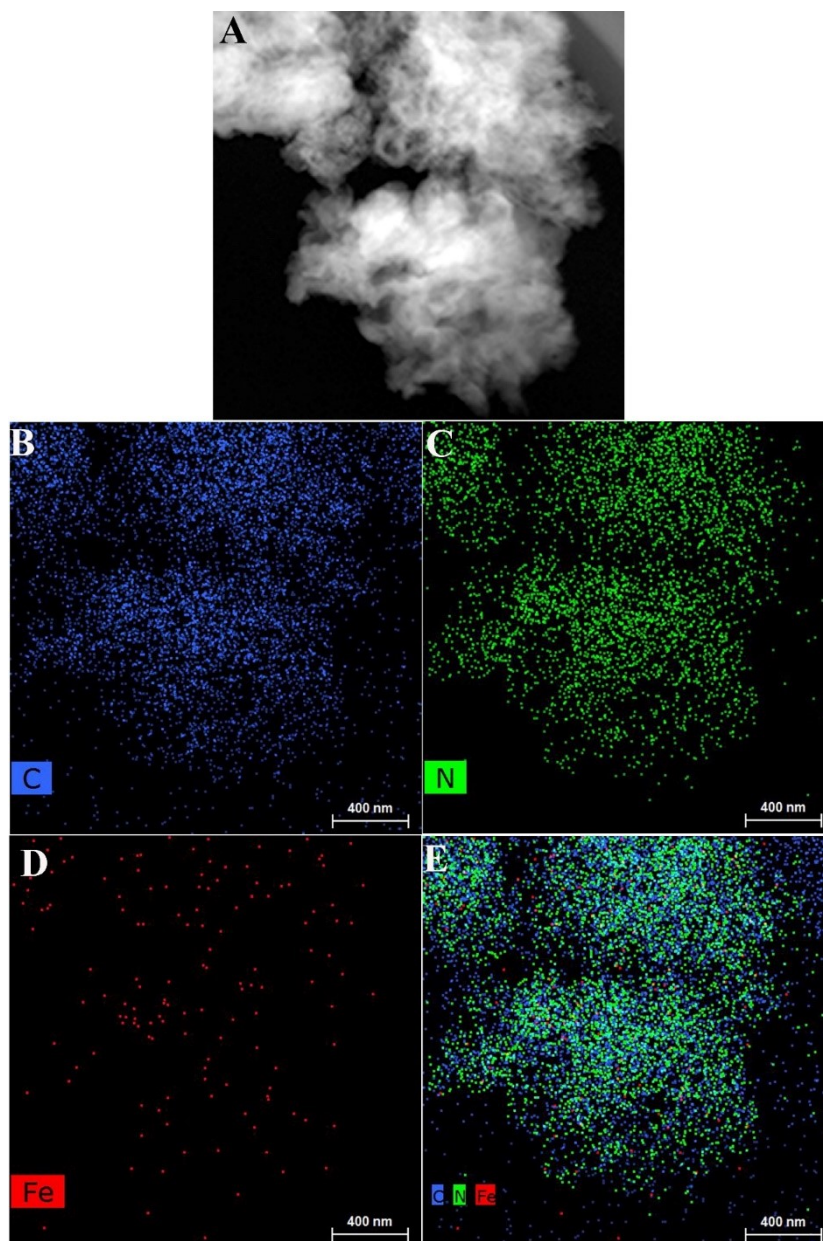


Figure S1. (A) The morphology and EDX-mapping images of C (B), N (C), Fe (D) and C, N , Fe elements for the as-prepared H-CN@Fe photocatalyst.

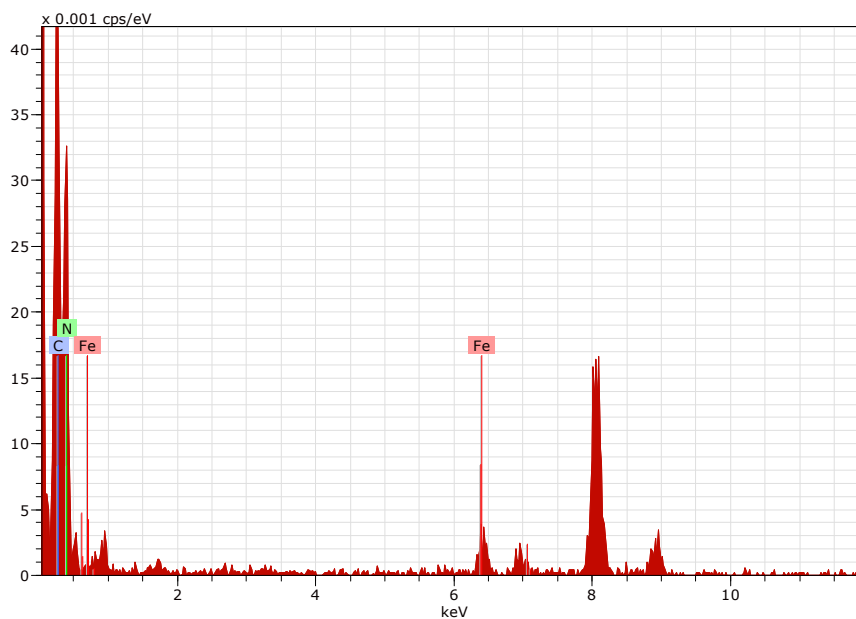


Figure S2. EDX patterns of as-prepared H-CN@Fe

Table S1. EDX element composition of as-prepared H-CN@Fe

Element	wt. %	at. %	Error
C-K	53.12	58.09	2.56
N-K	43.96	41.22	2.27
Fe-K	2.92	0.69	0.34

Table S2. The fitting results of EIS curves for CN, CN@Fe, H-CN, H-CN@Fe. R_s and R_{ct} represents the solution resistance and the charge transfer resistance across the electrode-solution interface.

Sample	R_s (Ω)	R_{ct} (Ω)
CN	4.39	6.22×10^4
CN@Fe	3.92	5.08×10^4
H-CN	3.79	4.58×10^4
H-CN@Fe	3.63	4.55×10^4

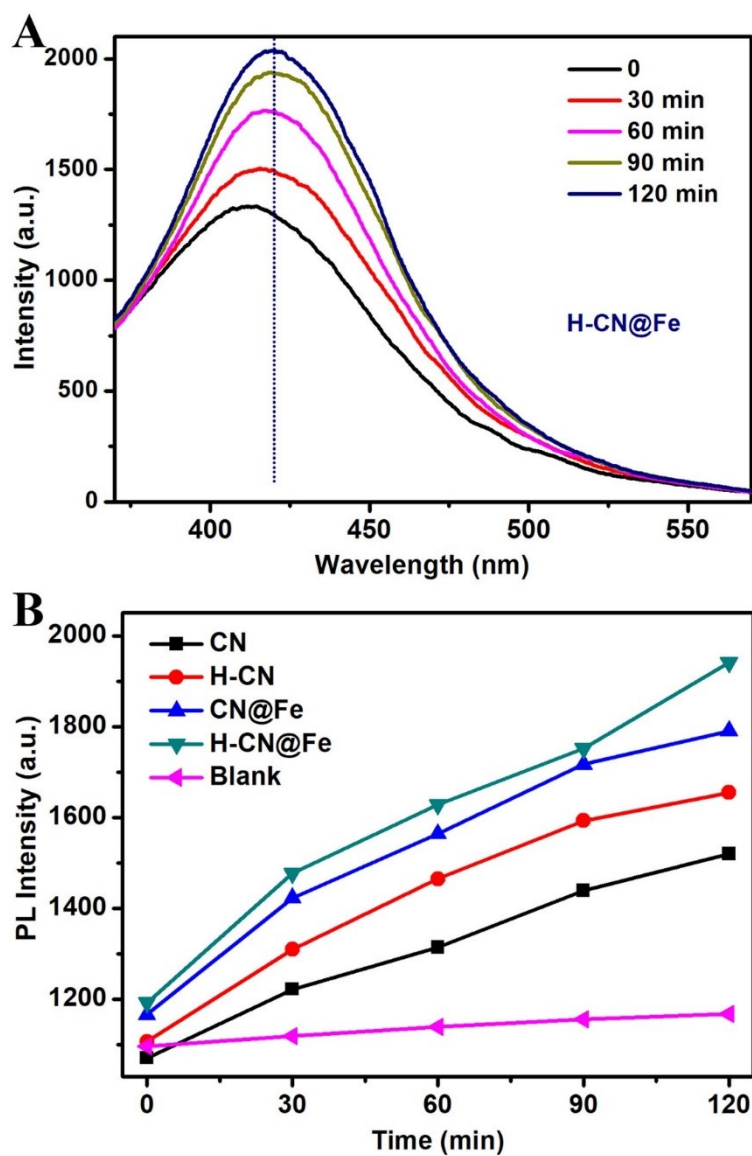


Figure S3. (A) Fluorescence spectra of TAOH solution over H-CN@Fe; (B) the PL intensity versus reaction time over CN, H-CN, CN@Fe and H-CN@Fe.

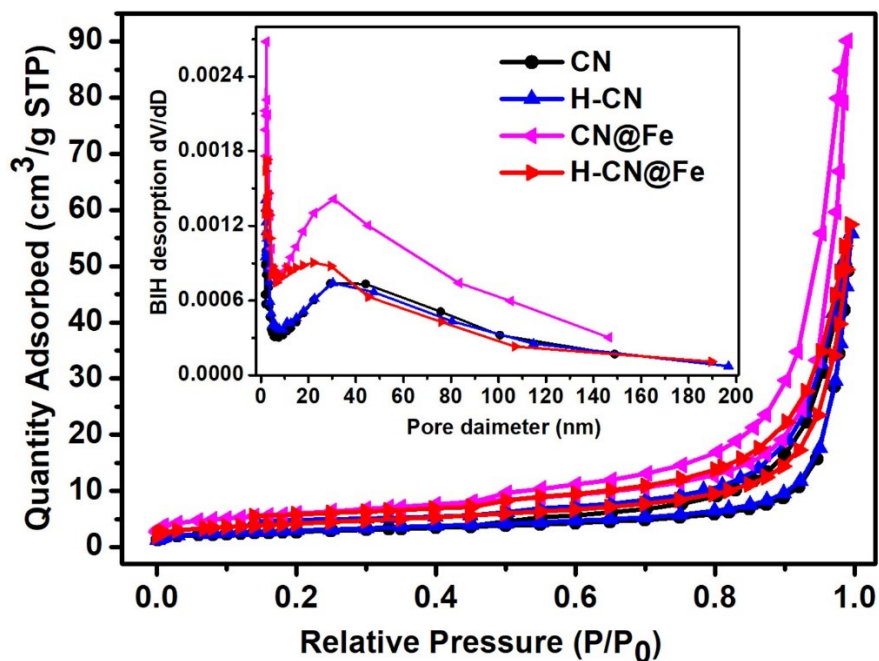


Figure S4. N₂ adsorption-desorption curves of CN, H-CN, CN@Fe and H-CN@Fe catalysts (inset: Barrett-Joyner-Halenda (BJH) based pore distribution analyses).

Table S3. The texture characteristics of prepared CN, H-CN, CN@Fe and H-CN@Fe catalysts.

Catalyst	S_{BET} (m ² /g)	V_p (cm ³ /g)	D_p (nm)
CN	9.74	0.078	30.62
H-CN	10.44	0.088	30.97
CN@Fe	21.10	0.14	26.26
H-CN@Fe	14.75	0.090	23.22